Polyoxoanion Occluded within Modified MCM-41: Spectroscopy and Structure

Wei Xu,[†] Qunhui Luo,[‡] Hsin Wang,[§] Lynn C. Francesconi,[‡] Ruth E. Stark,[§] and Daniel L. Akins*,[†]

Center for Analysis of Structures and Interfaces (CASI), Department of Chemistry, The City College of The City University of New York (CUNY), New York, New York 10031, Department of Chemistry, Hunter College of CUNY, New York, New York 10021, and Department of Chemistry, The College of Staten Island of CUNY, New York, New York 10314

Received: August 12, 2002; In Final Form: November 1, 2002

Polyoxoanions have enormous potential as drug delivery hosts, as catalysts, as agents for sequestering nuclear waste heavy metals, and as luminescent materials for laser and optical devices applications. We report the encapsulation of the polyoxoanion $[Eu(H_2O)_3(\alpha\text{-}1\text{-}P_2W_{17}O_{61})]^{7-}$ within Mobil crystalline material (MCM)-41. For proper host−guest interaction, it was necessary to functionalize the surface walls of MCM-41 through use of a silylation reagent, specifically, (aminopropyl)triethoxysilane. A stable and integrated $[Eu(H_2O)_3(\alpha\text{-}1\text{-}P_2W_{17}O_{61})]^{7-}$ polyoxoanion was shown to be formed inside the channels of modified MCM-41. X-ray diffraction, ^{29}Si magic angle spinning (MAS) NMR, UV−vis absorption, emission and excitation spectra, and Raman scattering measurements have been used to structurally characterize the various products. Cross-polarization ^{29}Si MAS NMR has been shown to better reveal the surface structural character of the modified MCM-41 than does regular ^{29}Si MAS NMR. We find (when compared to bulk polyoxoanion) that the Raman spectrum of the polyoxoanion/MCM-41 composite system exhibits red shifts for the symmetric stretching (ν_s) of the W−O_t (where O_t represents a terminal oxygen) and P−O−W bands. These latter observations are interpreted as suggesting that electrostatic interaction between the negative-charged terminal oxygen (O_t) of the polyoxoanion and the $-NH_3^+$ terminal functional group, associated with the silylation agent on the walls of MCM-41, leads to an increase in the lengths of adjacent W−O and P−O bonds. Given the shape and dimensions of the polyoxoanion and the diameter of the pores in MCM-41, as well as the effects of encapsulation on emission and Raman spectra, we conclude that the anion (i) is encapsulated with its long axis parallel to the pore axis and (ii) couples to the surface through interaction with terminal oxygens that are not directly bonded to the europium atom.

I. Introduction

Lanthanide and actinide derivatives of the monovacant, lacunary Wells−Dawson polyoxoanion $[P_2W_{17}O_{61}]^{10-}$ ligand have attracted great interest because of their potential applications in catalysis, medicine, and nuclear waste treatment. Moreover, europium-incorporated complexes have excited interest because of their structural and luminescence properties and with their potential use in lasers and luminescent materials. The europium/Wells−Dawson compound, in particular, has potential applications because of its photoluminescent properties, e.g., millisecond lifetime, strong emission with narrow full width at half-maximum (fwhm), large stokes shifts, and excellent solubility, as previously reported.[1]

A modest amount of work on the encapsulation of europium complexes within molecular sieves has been reported to date. In particular, occluded $[Eu(bpy)_2]^{3+}$ within Y zeolite has been found to be highly luminescent and stable and is suggested as a new luminescent material (i.e., phosphor).[2] More recently, Xu et al.[3] reported the incorporation of $Eu(TTA)_4C_5H_5NC_{16}H_{33}$ into surface-modified Mobil crystalline material (MCM)-41. An obvious disadvantage of this latter work is that the organic ligands used are expensive and the procedure for their preparation is tedious. Therefore, inexpensive, stable, and easily prepared polyoxometalate inorganic complexes, for example, as mentioned above, the europium/Wells−Dawson polyoxoanion, are particularly good candidates as perspective new luminescent materials.

To lend robustness and manipulability to the emitting species, a host material is to be sought. An obvious choice is MCM-41. This molecular sieve material (i.e., MCM-41) has one-dimensional pores that are highly uniform in size and a hexagonal-extended structural symmetry.[4,5] Through the use of different surfactants, the pore size of MCM-41 can be tailored in the range from 2 to 6 nm. In our laboratory, we have extensive experience in forming composite structures by encapsulating various molecules within MCM-41 as well as other siliceous materials, as shown by our earlier research efforts, which include the encapsulation of aggregated porphyrin (TSPP), cyanine dyes, and semiconductor nanoparticles within MCM-41 and SBA-15.[6−9] In the present work, we extend our prior efforts with the aims of creating composite, highly photoluminescent, and catalytic materials. We report here the encapsulation of $[Eu(H_2O)_3(\alpha\text{-}1\text{-}P_2W_{17}O_{61})]^{7-}$ (hereinafter referred to as Euα1) within modified MCM-41. Figure 1 depicts the structure of Euα1: the accepted sizes are ca. 10 and 20 Å for the minor and major dimensions, respectively. To promote the occlusion of Euα1, it was necessary to modify the interior structure of the mesoporous aluminosilicate through use of an alkoxysilane

[†] The City College of The City University of New York (CUNY).
[‡] Hunter College of CUNY.
[§] The College of Staten Island of CUNY.

10.1021/jp0267499 CCC: $25.00
Published on Web 12/12/2002

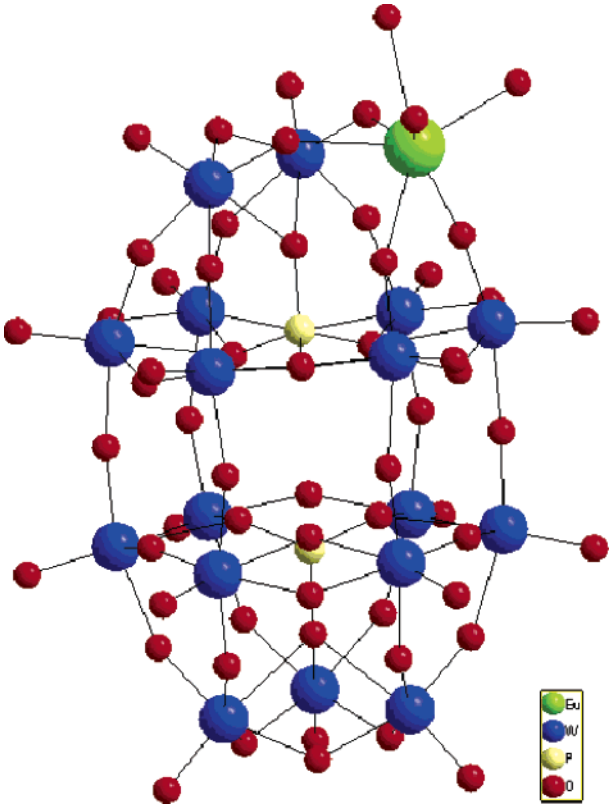

Figure 1. Ball and stick structure of the polyoxoanion. Note all of the terminal oxygens at the outer surface of the anion have a negative charge.

silylation reagent, in our present effort, (aminopropyl)triethoxysilane (APTES; $NH_2-(CH_2)_3-Si-(C_2H_5O)_3$), to satisfy guest−host electrostatic interaction through control of the ambient pH. The structural properties of both modified MCM-41 and the composite material are investigated using several techniques, including cross-polarization (CP) MAS ^{29}Si NMR, absorption and fluorescence spectroscopies, and Raman scattering. We deduce that the well-organized, stable, and highly luminescent composite material that we have developed may have applications for flat-panel display devices and as phosphors.

II. Experimental Section

Synthesis of MCM-41 and Polyoxoanion (Euα1). Polycrystalline powders of the mesostructural aluminosilicate MCM-41 were prepared by using cetyltrimethylammonium bromide (CTAB) as the template.[4,5] Briefly, Na_2SiO_3 (Aldrich, ∼27% SiO_2) solution and a calculated amount of $NaAlO_2$ (Alfa) solution (Si/Al = 10) were added to CTAB (Aldrich) solution according to the molar composition ratio $5SiO_2$:0.25-Al_2O_3:CTAB:$610H_2O$. The pH was lowered to 11 with 2 M H_2SO_4, and the mixture was stirred for >3 h at about 318 K. Then, the temperature was raised to 373 K, and the reaction was allowed for 72 h in a Teflon-lined autoclave. The resultant precipitate was filtered, washed thoroughly with distilled water, and calcined in air at 773 K to obtain the final product MCM-41. As regards the polyoxoanion, details are not presented here, but a reference is given for the recipe followed.[1]

Modification of MCM-41. Several detailed reports have been recently published describing MCM-41 surface modifications using alkoxysilane coupling agents.[10] For our studies, the modified MCM-41 was prepared according to a procedure detailed in ref 10a. Briefly, about 1.5 g of the calcined MCM-41 was mixed with a chloroform solution of APTES (100 mL, 0.2 M) and stirred overnight at room temperature. The precipitate was filtered and washed with chloroform and dichloromethane.

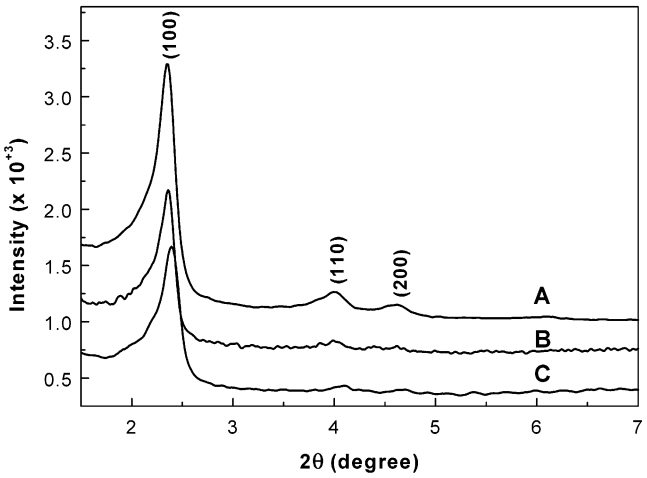

Figure 2. XRD patterns of (A) calcined MCM-41, (B) modified MCM-41, and (C) Euα1/MCM-41.

Formation of Euα1/MCM-41 Composite. A typical ion exchange preparation of a Euα1/MCM-41 composite involved stirring a mixture of 100 mg of modified MCM-41, 100 mg of Euα1, and 20 mL of distilled water for over 24 h at room temperature with the pH held at about ca. 5 using 2 M H_2SO_4. The suspension was then centrifuged, and the supernatant aqueous solution was decanted. The white powder (hereinafter designated Euα1/MCM-41) was washed several times with pH 5 water to remove Euα1 from the external surface and then dried in air.

Instrumentations. Steady state emission and excitation spectra were acquired using a SPEX Fluorolog-τ2 spectrofluorometer. The X-ray diffraction (XRD) instrument used was a Rigaku diffractometer, using Cu $K\alpha_1$ (0.154 nm) X-rays, typically run at a voltage of 40 kV and current of 30 mA.

Solid state ^{29}Si MAS NMR spectra were obtained on a Varian 300 spectrometer. Samples were spun at a frequency of 4 kHz in a MAS zirconia rotor. CP MAS ^{29}Si NMR was conducted at a frequency of 63 MHz for ^{29}Si and a frequency of 59 MHz for ^{1}H; the software utilized was Spinworks, version 1.2. The contact time used in this study was 8 ms, which was sufficiently long to permit full CP for different silicon atoms. Spectral contributions from silicons deeper in the lattice were strongly discriminated against in the CP experiment due to their prohibitively long Si−H distances, a subject that will be discussed below. As a consequence, the intensities of the signals from the isolated and geminal silanols and the attached silane groups are believed to be reliable and valid. MAS without CP was conducted at low power at a frequency of 57 MHz for ^{29}Si, with a relaxation delay of 2 s. The reference sample used was tetramethylsilane (TMS).

Raman spectra of pure solid state Euα1 and composite Euα1/MCM-41 were excited with laser radiation of wavelength 488 nm from a Coherent Innova 200 argon-ion laser. The excitation power was maintained at 100 mW, and the Raman scattering was collected and dispersed by a Spex 1877, 0.6 m spectrometer. A cooled (140 K) Spex Spectrum-1 CCD camera was coupled to the spectrometer and used as the detector.

III. Results and Discussion

XRD patterns of pristine calcined MCM-41, modified MCM-41, and the polyoxoanion-incorporated composite (Euα1/MCM-41) are shown in Figure 2. Our prior work,[6] combined with the

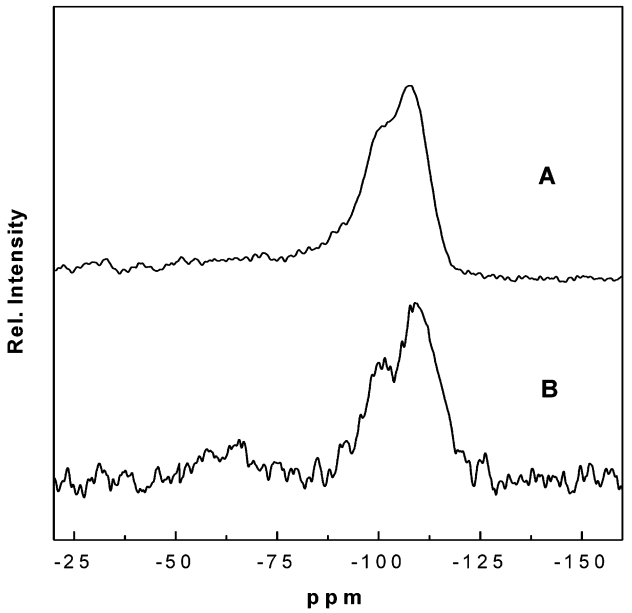

Figure 3. MAS ^{29}Si NMR spectra of (A) calcined MCM-41 and (B) modified MCM-41.

result of nitrogen isotherm (not shown), demonstrated that after the silylation reaction—and likely formation of a monolayer of silylation product on the surface walls—the pore size of modified MCM-41 was narrowed from ca. 29 to ca. 21 Å. An opening of ca. 21 Å is anticipated to be sufficiently large to allow the polyoxoanion Euα1 (of dimensions ~10 Å in diameter and ~20 Å in length) to be incorporated into the modified MCM-41. The XRD patterns of the three samples show strong (100) peaks and proportional (110) and (200) peak intensities, suggesting that the incorporation of polyoxoanion in the channels does not affect the framework integrity of modified MCM-41. It is also to be noted that the (100) peak gradually shifts to higher angles both with functionalization of MCM-41 and loading of polyoxoanion Euα1, indicating an effective diminution of MCM-41 pore diameter, which can be understood in terms of excluded volumes associated with the silylation of the MCM-41 surface walls and the presence of the polyoxoanions within the pores.

The (normal) ^{29}Si MAS NMR spectra of calcined MCM-41 and modified MCM-41 are shown in Figure 3 (parts A and B, respectively). For both samples, three peaks (with location near −110, −100, and −92 ppm), corresponding to Q^4, Q^3, and Q^2 (that will be discussed in detail below), are identified by multipeak curve fitting. Essentially the same relative peak intensities shown in Figure 3 have been found regardless of sample, indicating that the spectra correspond to bulk silicon rather than interfacial silicon. To enhance NMR signals associated with the interior surface of the modified MCM-41, we exploited CP NMR (i.e., CP/MAS NMR), which amplifies signals from chemically bonded atoms, in the present case protons and silicon atoms.[11] More specifically, the ^{1}H and ^{29}Si CP experiment restricts detection of an NMR signal to silicon nuclei that are near protons, the latter existing at or near the surface. The determinations using the CP approach are discussed below.

^{29}Si CP/MAS NMR is a sensitive and reliable technique for qualitative and quantitative determination of SiOH groups on solid surfaces. Figure 4 shows the ^{29}Si CP/MAS NMR spectra for calcined MCM-41 (part A) and modified MCM-41 (part B) samples. Multipeak curve fitting indicates that for the calcined sample without silylation, three peaks can be identified in the vicinity of −100 ppm. According to Maciel et al.,[11b] the three

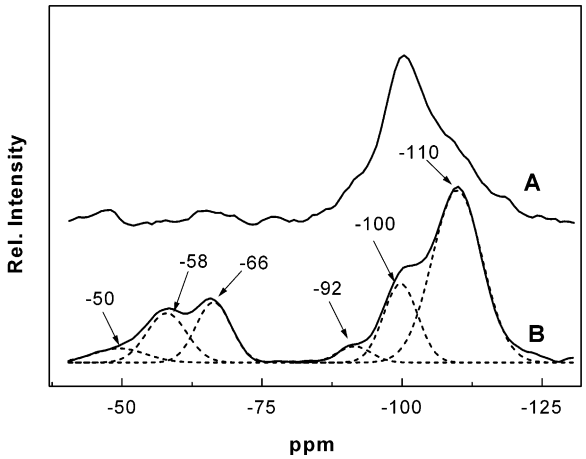

Figure 4. CP/MAS ^{29}Si NMR spectra of (A) calcined MCM-41 and (B) modified MCM-41. Multipeak curve fitting result for curve B is also illustrated. Various peaks are attributed to the siloxane bonding scheme as described in the text.

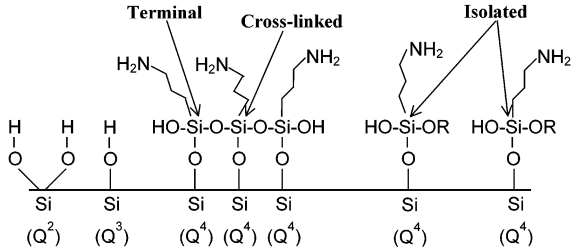

Figure 5. Schematic conformations of the functionalized monolayer on the surface. Representation is mimicked after schematic representation presented in ref 10c.

peaks are composed of a low intensity peak at −92 ppm, which corresponds to surface silicon atoms with two siloxane bonds and two geminal silanol groups (either single or hydrogen-bonded), represented as $(SiO)_2$*$Si(OH)_2$ and labeled in Figure 5 as a Q^2 silicon; a peak at −100 ppm attributed to surface silicon atoms with three siloxane bonds and one (isolated) silanol group, represented as $(SiO)_3$*SiOH and labeled in Figure 5 as a Q^3 silicon; and a resonance at −110 ppm attributed to surface silicon atoms with four siloxane bonds, i.e., $(SiO)_4$*Si, and labeled in Figure 5 as a Q^4 silicon.

For the silated sample, i.e., modified MCM-41, one observes a change in relative intensities of the resonances in the vicinity of −100 ppm when compared to the signals for the pristine calcined sample. In particular, the relative intensity for the Q^3 silicon resonance labeled as −100 ppm undergoes a significant diminution as compared to the Q^4 silicon resonance at ca. −110 ppm. This difference in relative intensity is attributable to reactions of surface SiOH groups with APTES that lead to the formation of more SiO bonds.

The additional peaks lying in the range from −50 to −80 ppm, as shown in part B of Figure 4, occur only for the silated sample; that is, the silicon atoms in the silylation reagent, as a result of chemically bonding to the surface of MCM-41, contribute to the appearance of three new peaks. The three resonances indicate three different environments for the siloxane groups in the functionalized monolayer. Similar to studies that involved monolayers formed using (trimethoxyl)mercaptopropylsilane (TMMPS) as the silylation reagent (ref 10c), the three resonances, as depicted in Figure 5, can be assigned as the following: (i) the resonance at ca. −50 ppm arises from isolated SiO_3 groups that are not bound to any neighboring

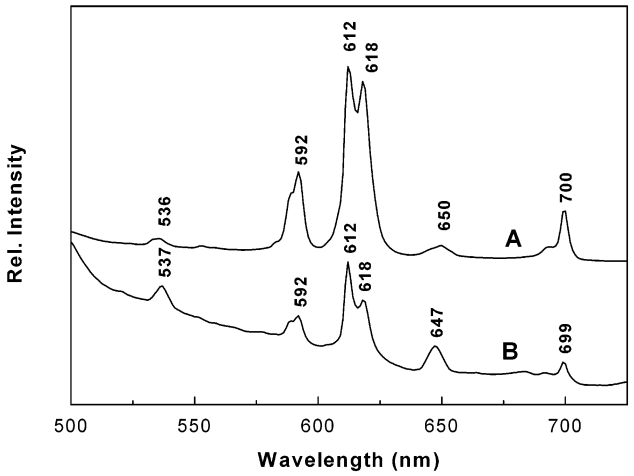

Figure 6. Emission spectra of (A) solid Euα1 and (B) composite Euα1/MCM-41, excited at 394 nm.

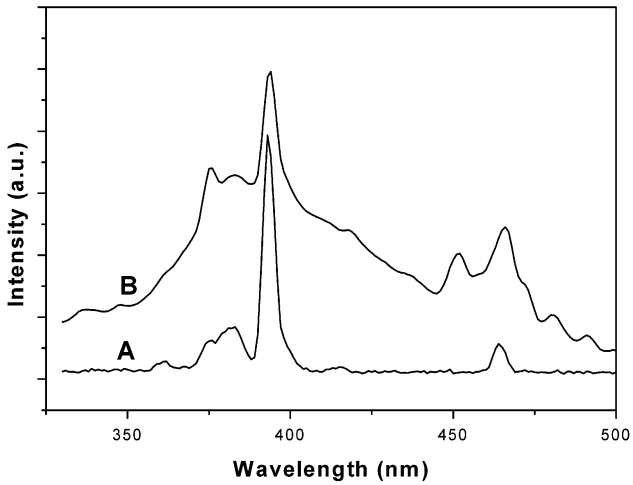

Figure 7. Excitation spectra of (A) solid Euα1 and (B) composite Euα1/MCM-41. Spectra were taken at 615 nm.

siloxanes, (ii) the resonance at ca. −58 ppm arises from terminal groups that are only bound to one neighboring siloxane, and (iii) the resonance at ca. −66 ppm arises from cross-linked groups that are bound to two neighboring siloxanes. It is to be noted that the NMR pattern for these three peaks is very similar to that of an approximately 76% relative surface coverage sample, rather than that of 25% coverage sample as reported in ref 10c, and deduced from the fact that among the three peaks, the dominant one is attributed to the cross-linked siloxane group. We estimate the surface coverage of the functionalized monolayer of mesoporous MCM-41 to be greater than 50%, through comparison with estimates reported in the literature (ref 10c).

It should be pointed out that the choice of a suitable pH for the solution is important for successful encapsulation of polyoxoanion in MCM-41. At lower pH, polyoxoanions can capture protons and form the neutral weak acid, which is not favorably incorporated into the MCM-41 channels because of the electrostatic interaction with positive-charged $-NH_3^+$ functional groups on the surface walls of modified MCM-41. However, at ca. pH 5, where the decomposition of polyoxoanion into smaller ions that occurs in basic medium is not favored, the incorporation of $[Eu(H_2O)_3(\alpha\text{-}1\text{-}P_2W_{17}O_{61})]^{7-}$ is promoted as a result of host−guest interaction between the negative-charged terminal oxygen and the interfacial $-NH_3^+$ terminal group.

Emission spectra of the pure solid state Euα1 and the composite Euα1/MCM-41 are shown in Figure 6. It is to be noted that the emission spectra for both samples are quite similar, indicating weak electrostatic interaction between the encapsulated polyoxoanion and the surface walls of MCM-41. This is to be expected given the large pore size (∼21 Å) of the functionalized MCM-41 that permits maintenance of the integrity of the structure of Euα1 (of approximate dimensions 10 Å middiameter and 20 Å length) and the integrated character of the composite. Indeed, the encapsulated Euα1 might be expected to exist in an environment somewhat similar to that in solution, i.e., little steric hindrance, and possess a similar spectrum (which, indeed, it does, although the solution spectrum is not provided here).

The two emission spectra shown in Figure 6 exhibit bands near 536 nm corresponding to $^5D_1 \rightarrow {}^7F_J$ transitions.[12] Also, in the spectra, there exist bands near 592 nm attributed to the $^5D_0 \rightarrow {}^7F_1$ transition, bands near 612 and 618 nm corresponding to the $^5D_0 \rightarrow {}^7F_2$ transition, a band near 647 nm corresponding to the $^5D_0 \rightarrow {}^7F_3$ transition, and a band near 699 nm corresponding to the $^5D_0 \rightarrow {}^7F_4$ transition.[12] It is to be noted that the forbidden transition $^5D_0 \rightarrow {}^7F_0$ that would appear at ca. 579 nm is not present in either of the spectra, indicating a lack of centrosymmetry for the Eu^{3+} ion, as is indicated by the structure of the polyoxoanion chromophore.

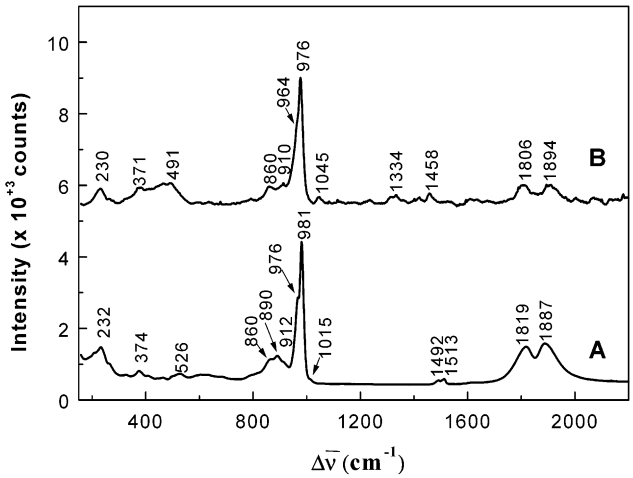

Figure 8. Raman spectra of (A) solid Euα1, integration time = 0.8 s and number of repetitions = 100, and (B) composite Euα1/MCM-41, integration time = 5 s and number of repetition = 100. Excitation wavelength of 488 nm and laser power nominally 100 mW. For the composite, a background subtraction was used that involved a 40 point segmented line fit to a positive signal that underlied the Raman scattering.

The excitation spectra of both solid state Euα1 and the composite Euα1/MCM-41 exhibit maximum intensities at ca. 394 nm, with the intrinsic absorption band for the composite Euα1/MCM-41 being somewhat broader (Figure 7; detection wavelength of 615 nm). Moreover, for the composite Euα1/MCM-41, the excitation spectrum is more complex, with additional absorption bands at 452, 472, 480, and 491 nm. Such an observation suggests that the polyoxoanion is located at varied sites within the channels of modified MCM-41 and exhibits what might be characterized as weak microenvironmental site perturbations.

Figure 8 shows Raman spectra of solid state Euα1 and the composite Euα1/MCM-41; similar Raman patterns occur in the two samples. Specifically, both spectra have vibration bands at ca. 230, 970 (a shoulder band), and 980 cm^{-1}, which, respectively, are assignable to a symmetrical stretch ν_s for the $W-O_t$ bond, where O_t represents terminal oxygen; an asymmetrical

stretch ν_{as} for the same W−O_t bond; and a symmetrical stretch ν_s for the P−O−W bond.[13,14] Relative weak bands at ca. 374 (860, 890, 912) and 1015 cm^{-1} are assigned to bending δ(W−O−W), symmetric stretching ν_s(W−O−P), and asymmetric stretching ν_{as}(W−O−P), respectively.[13] It is to be noted that bands at ca. 1819 and 1887 cm^{-1} are likely overtones of the ν_s and ν_{as}(W−O_t) fundamental bands at 967 and 981 cm^{-1}, respectively. One finds that certain bands in the Raman spectra shown in Figure 8 of the composite, vis-à-vis the respective bands for solid state Euα1, show red shifts: e.g., the 230 and 232 for ν_s(W−O_t) and the 976 and 981 for ν_s(P−O−W), respectively. On the basis of their assignments above, an immediate explanation for the band shifts and their direction is that host−guest interaction between negatively charged electrons of the terminal oxygens and the $-NH_3^+$ terminal functional group on the wall of MCM-41, although weak, can be expected to promote redistribution of local electrons on the polyoxoanion. The redistribution can be expected to decrease the electron densities of adjacent O, P, and W atoms, leading to an increase in bond lengths of W−O and P−O, with an associated red shift.

With regard to optical spectra insight into the orientation of the polyoxoanion in the MCM-41 host, we are led to the conclusion, based on the emission and Raman results, that the host−guest interaction involves mainly the negatively charged terminal oxygens and not the oxygen chemically bonded to the europium atom. This conclusion is based on the presumption that interaction with the oxygens bonded to europium would substantially alter the energy states of the d electrons of the europium atom, resulting in, especially where emission is concerned, detectable shifts in energy states. We conclude, therefore, that the polyoxoanion compound is oriented longitudinally along the channels, in agreement with steric effect assumptions but (from optical spectra) that the europium atom is positioned away from the surface wall.

IV. Conclusion

The conflation of XRD, ^{29}Si MAS NMR, UV−vis absorption, emission, excitation, and Raman scattering measurements is interpreted as indicating that we have formed encapsulated polyoxoanion $[Eu(H_2O)_3(\alpha\text{-}1\text{-}P_2W_{17}O_{61})]^{7-}$ within the pores of modified MCM-41. To facilitate the incorporation of negative-charged polyoxoanion, we found it necessary to functionalize the wall of the silicate using an alkoxysilane reagent and to control the pH during the preparation so as to meet the requirement for host−guest interaction. CP ^{29}Si MAS NMR was able to characterize the surface structural interaction, while normal ^{29}Si MAS NMR did not differentiate between species and bonds at the surface. On the basis of emission, excitation, and Raman scattering measurements, we deduce that the structural integrity of $[Eu(H_2O)_3(\alpha\text{-}1\text{-}P_2W_{17}O_{61})]^{7-}$ is maintained inside the channels of modified MCM-41 although some weak microenvironmental perturbations exist. Furthermore, by way of comparison of Raman band positions, we suggest that the incorporation of $[Eu(H_2O)_3(\alpha\text{-}1\text{-}P_2W_{17}O_{61})]^{7-}$ is implemented by host−guest interaction between the negative-charged terminal oxygen and the $-NH_3^+$ terminal functional group on the wall of MCM-41, at an appropriate pH. Because of its well-organized stable structure and luminescent property, such a composite might represent a new material with potential applications as a photoluminescent device or phosphor.

Acknowledgment. The NSF supported this work, in part, through the following awards: IGERT program under Grant DGE-9972892; MRSEC program under Grant No. DRM-9809687; and Army Research Office of DoD under Agreement No. DAAD19-01-1-0759. D.L.A. would also like to thank a colleague (Dr. Maria C. Tamargo) for use of her XRD instrument.

References and Notes

(1) Bartis, J.; Dankova, M.; Lessmann, J. J.; Luo, Q.-H.; Horrocks, W. DeW., Jr.; Francesconi, L. C. *Inorg. Chem.* **1999**, *38*, 1042.

(2) Rosa, I. L. V.; Serra, O. A.; Nassar, E. J. *J. Lumin.* **1997**, *72*, 532.

(3) Xu, Q.; Li, L.; Liu, X.; Xu, R. *Chem. Mater.* **2002**, *14*, 549.

(4) Kresge, C. T.; Leonowicz, M. E.; Roth, W. J.; Vartuli, J. C.; Beck, J. S. *Nature* **1992**, *359*, 710.

(5) Beck, J. S.; Vartuli, J. C.; Roth, W. J.; Leonowicz, M. E.; Kresge, C. T.; Schmitt, K. D.; Chu, C. T.-W.; Olsen, D. H.; Sheppard, E. W.; McCullen, B.; Higgins, J. B.; Schlenker, J. L. *J. Am. Chem. Soc.* **1992**, *114*, 10834.

(6) Xu, W.; Guo, H.; Akins, D. L. *J. Phys. Chem. B* **2001**, *105*, 1543.

(7) Xu, W.; Guo, H.; Akins, D. L. *J. Phys. Chem. B* **2001**, *105*, 7686.

(8) Xu, W.; Akins, D. L. *J. Phys. Chem. B* **2002**, *106*, 1943.

(9) Xu, W.; Liao, Y.; Akins, D. L. *J. Phys. Chem. B* **2002**, *106*, 11127.

(10) Liu, C.-J.; Li, S.-G.; Pang, W.-Q.; Che, C.-M. *Chem. Commun*. **1997**, *1*, 78. (b) Mercier, L.; Pinnavaia, T. J. *Adv. Mater*. **1997**, *9*, 500. (c) Feng, X.; Fryxell, G. E.; Wang, L. Q.; Kim, A. Y.; Liu, J.; Kemner, K. M. *Science* **1997**, *276*, 923. (d) Liu, J.; Feng, X.; Fryxell, G. E.; Wang, L. Q.; Kim, A. Y.; Gong, M. *Adv. Mater.* **1998**, *10*, 161. (e) Cauvel, A.; Renard, G.; Brunel, D. *J. Org. Chem*. **1997**, *62*, 749. (f) Brunel, D.; Cauvel, A.; Fajula, F.; DiRenzo, F. *Stud. Surf. Sci. Catal*. **1995**, *97*, 173. (g) Sutra, P.; Brunel, D. *Chem. Commun*. **1996**, 2485. (h) Bellocq, N.; Brunel, D.; Lasperas, M.; Moreau, P. *Stud. Surf. Sci. Catal*. **1997**, *108*, 485. (i) Subba Rao, Y. V.; De Vos, D. E.; Bein, T.; Jacobs, P. A. *Chem. Commun*. **1997**, 355. (j) Subba Rao, Y. V.; De Vos, D. E.; Jacobs, P. A. *Angew. Chem., Int. Ed. Engl*. **1997**, *36*, 2661. (k) Diaz, J. F.; Balkus, K. J., Jr.; Bedioui, F.; Kurshev, V.; Kevan, L. *Chem. Mater*. **1997**, *9*, 61.

(11) Sindorf, D. W.; Macier, G. E. *J. Am. Chem. Soc.* **1983**, *105*, 1487. (b) Sindorf, D. W.; Maciel, G. E. *J. Am. Chem. Soc*. **1981**, *103*, 4263.

(12) Archer, R. D.; Chen, H.; Thompson, L. C. *Inorg. Chem.* **1998**, *37*, 2089.

(13) Rocchiccioli-Deltcheff, C.; Thouvenot, R. *J. Chem. Res., Synop.* **1977**, 46.

(14) Raţiu, C.; Tomşa, A.; Koutsodimou, A.; Falaras, P.; Budiu, T. *Polyhedron* **2002**, *21*, 353.